

# Electron Temperature and Electron Density of Underwater Pulsed Discharge Plasma Produced by Solid-State Pulsed-Power Generator

journal or publication title	IEEE TRANSACTIONS ON PLASMA SCIENCE
volume	35
number	3
page range	614-618
year	2007-06
URL	<a href="http://hdl.handle.net/2298/3503">http://hdl.handle.net/2298/3503</a>

doi: 10.1109/TPS.2007.896965

# Electron Temperature and Electron Density of Underwater Pulsed Discharge Plasma Produced by Solid-State Pulsed-Power Generator

Takao Namihira, *Senior Member, IEEE*, Shunsuke Sakai, Takahiro Yamaguchi, Kunihiro Yamamoto, Chiemi Yamada, Tsuyoshi Kiyon, Takaishi Sakugawa, Sunao Katsuki, *Member, IEEE*, and Hidenori Akiyama, *Fellow, IEEE*

**Abstract**—A pulsed discharge produced underwater has been an attractive method to treat waste water. For the optimization and realization of the water treatment system utilizing underwater pulsed discharge, modeling analysis could be one of the essential works. However, there is still no simulation work about the underwater pulsed discharge due to the lack of knowledge about its characteristic parameters such as electron temperature, electron density, and so on. In this paper, the temperature and the electron density in a pulsed discharge plasma produced underwater are measured and presented. A magnetic pulse compressor (MPC) was developed and used to create the electrical discharge in water. The developed MPC is all-solid state and is, therefore, a maintenance-free generator. To define the temperature and the electron density in an underwater pulsed discharge plasma, two kinds of spectroscopic measurements, called the line-pair method and Stark broadening, were carried out. According to the experimental results, the temperature and the electron density in the pulsed discharge plasma between point-plane electrodes immersed in water are determined to be 15 000 K and  $10^{18}/\text{cm}^3$ , respectively.

**Index Terms**—Discharge plasma, electron density, electron temperature, pulsed power, streamer discharge, underwater discharge.

## I. INTRODUCTION

IN THE LAST decade, pulsed-power technology has been developed quickly and can cause an electrical discharge in liquid medium, such as water and dielectric oil [1]. The discharge creates certain physical phenomena in the liquid medium, such as an intense electric field at the tips of a discharge column, radical formation in the discharge channel, ultraviolet radiation from discharge emission, and shockwave generation at the boundary between the plasma and liquid medium [2]. These phenomena are very attractive for treatment of polluted water and harmful waterborne bacteria. It is clear that modeling studies of discharge phenomena can give a

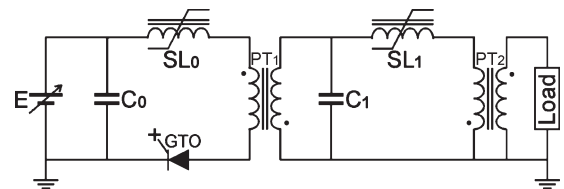


Fig. 1. Equivalent circuit of the MPC used in this paper.  $E$ : 4 kV<sub>max</sub>.  $C_0$ : 6.6  $\mu\text{F}$ ,  $SL_0$ : Saturable inductor,  $PT_1$ : 4 : 24,  $C_1$ : 200 nF,  $SL_1$ : Saturable inductor,  $PT_2$ : 1 : 5.

detailed information without experiments in order to realize a variety of industrial, medical, and environmental applications based on underwater pulsed discharge. However, there is no literature about simulation work of underwater pulsed discharge because of the lack of knowledge about the parameters of an underwater pulsed discharge plasma. In this paper, the temperature ( $T_p$ ) and electron density ( $N_e$ ) of a pulsed discharge plasma underwater were defined by an analysis of optical emission from the discharge. The line-pair method and Stark broadening of  $H_\alpha$  spectral analysis were utilized to compute  $T_p$  and  $N_e$ , respectively.

## II. EXPERIMENTAL SETUP AND CALCULATION THEORY

### A. Pulsed-Power Generator, Discharge Electrode, and Spectroscopic Equipment

Fig. 1 shows the electrical circuit of the magnetic pulse compressor (MPC) developed and used in this paper. The maximum charge energy for  $C_0$  ( $= 6.6\mu\text{F}$ ) of the developed MPC is approximately 40 J/pulse at 3.5-kV charging voltage. The developed MPC operates as follows. First, the dc power supply charges  $C_0$  to the set voltage, and then, the gate-turn-off (GTO) thyristor is turned on. After the GTO is fully turned on, the saturable inductor  $SL_0$  saturates, and the main discharge current from  $C_0$  flows in the primary circuit of the first pulse transformer  $PT_1$  (ratio, 4 : 24). At this time, the stored energy in  $C_0$  is transferred into  $C_1$  through  $PT_1$ . After the energy transfer from  $C_0$  to  $C_1$ , the saturable inductor  $SL_1$  is saturated, and the discharge current from  $C_1$  flows in the primary circuit of the second pulse transformer  $PT_2$  (ratio, 1 : 5). At this time, the stored energy in  $C_1$  is transferred to a load through  $PT_2$ . Finally, a positive pulse voltage is generated in the secondary circuit of  $PT_2$ . In the developed MPC, the material for all magnetic cores

Manuscript received July 19, 2005; revised November 4, 2006.

T. Namihira, S. Sakai, C. Yamada, T. Kiyon, T. Sakugawa, S. Katsuki, and H. Akiyama are with the Graduate School of Science and Technology, Kumamoto University, Kumamoto 860-8555, Japan (e-mail: namihira@cs.kumamoto-u.ac.jp).

T. Yamaguchi is with Ishikawajima-Harima Heavy Industries Company, Ltd., Kanagawa 235-8501, Japan.

K. Yamamoto is with Toray Industries, Inc., Shiga 520-0842, Japan.

Color versions of one or more of the figures in this paper are available online at <http://ieeexplore.ieee.org>.

Digital Object Identifier 10.1109/TPS.2007.896965

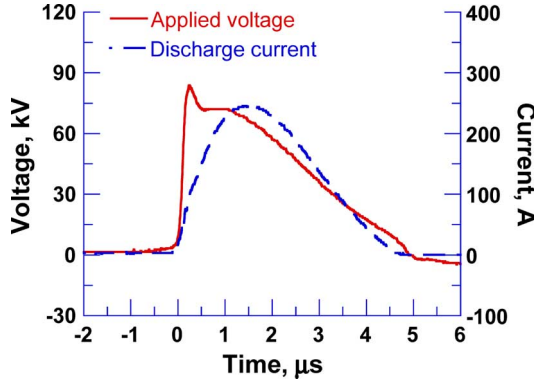


Fig. 2. Applied voltage and discharge current into the discharge electrode.

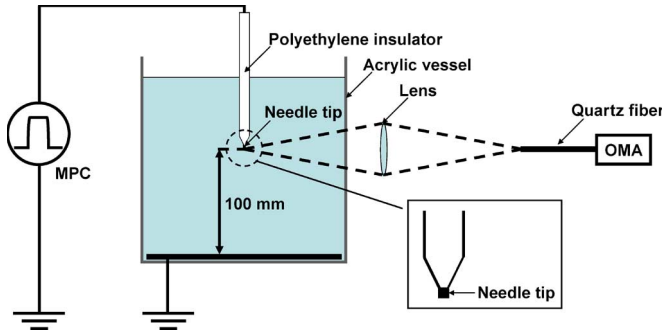


Fig. 3. Experimental setup.

was FINEMET (FT-3H, Hitachi Metals, Japan). The developed MPC, having no mechanical or spark gap discharge switches, was constructed using all-solid state devices and, therefore, maintenance-free. Fig. 2 shows the typical waveform of the output voltage and current from the MPC for the discharge electrode shown in Fig. 3. As observed in Fig. 2, the pulsewidth of the output voltage from the developed MPC is approximately  $3 \mu\text{s}$ .

Fig. 3 shows the experimental setup. The needle-to-plane electrodes, which were immersed in tap water (Conductivity:  $250 \mu\text{S}/\text{cm}$ ), were used as the discharge electrodes in this experiment. The radius of curvature of the needle tip was  $30 \mu\text{m}$ . The needle, except the tip, was coated with a polyethylene insulator to enhance the electric field at the tip of the needle electrode. In the experiments, the distance between the tip of the needle electrode and the plane electrode was fixed at  $100 \text{ mm}$ . The developed MPC was connected to the needle and plane electrodes, and  $C_0$  of the MPC was charged up to  $2.0$ ,  $2.8$ , and  $3.5 \text{ kV}$ . The applied voltage and the discharge current through the needle-to-plane electrode gap were measured using a voltage divider (EP-100K, Pulse Electronic Engineering Company, Japan) and a current transformer (Model 110A, Pearson Electronics, Japan), respectively. An oscilloscope (HP54542A, Hewlett-Packard, USA) recorded the signal from the measurement devices. For the spectroscopic measurements, the emission from the underwater pulsed discharge in the vicinity of the tip of the needle electrode was transmitted to the optical multichannel analyzer (Macs 320, Atago Bussan, Japan) using a collective lens ( $f = 100$ ) and a quartz fiber. The optical multichannel analyzer with  $0.18 \text{ nm}$  of spectral

resolution was triggered and gated by a pulse/delay generator (DG535, Stanford Research Systems, USA). The pulse/delay generator facilitated the synchronization between the developed MPC and the optical multichannel analyzer. It is noted that the optical multichannel analyzer has a self-calibrating system using a Hg lamp and is calibrated prior to conducting the experiments.

### B. Calculation of Plasma Temperature and Electron Density

Optical emission spectroscopy is a suitable diagnostic to obtain physical information about a discharge plasma, such as composition, temperature, and electron density. In this paper, the temperature and the electron density in the discharge plasma produced underwater were calculated based on the results of two kinds of spectroscopic measurements. One is the line-pair method for the calculation of the plasma temperature. The other is based on Stark broadening of the  $H_\alpha$  line emitted from the discharge plasma, which interacts with the electron density in the discharge plasma.

The temperature of the discharge plasma induced in water was given by the following equation [3]:

$$\ln\left(\frac{I\lambda}{Ag_u}\right) = \frac{1}{kT_p}E_u + C \quad (1)$$

where  $I$ ,  $\lambda$ ,  $A$ ,  $g_u$ ,  $k$ ,  $T_p$ ,  $E_u$ , and  $C$  are the emission intensity, its wavelength in nanometer, its transition probability in  $10^8/\text{s}$ , its statistical weight, Boltzmann's constant in electronvolts per kelvin, plasma temperature in kelvin, upper energy level in electronvolts, and a constant. In this paper, four atomic emission lines from copper, the anode needle electrode material, were observed and were used for the calculation of plasma temperature with the Boltzmann's plot. The values of  $\lambda$ ,  $A$ ,  $g_u$ , and  $E_u$  for copper emissions were from [3].

The electron density was calculated by the following equation [4]:

$$N_e = 8.02 \times 10^{12} \times \left[ \frac{\Delta\lambda_{H_\alpha\text{StarkFWHM}}}{\alpha_{H_\alpha\text{StarkFWHM}}} \right]^{0.63} \quad (2)$$

where  $N_e$ ,  $\Delta\lambda_{H_\alpha\text{StarkFWHM}}$ , and  $\alpha_{H_\alpha\text{StarkFWHM}}$  are the electron density in per cubic centimeter, full width at half maximum (FWHM) of  $H_\alpha$  spectral broadened by the Stark effect in nanometer, and the Stark constant which was given in [5]. Fig. 4 shows the dependence of  $N_e$  on  $\Delta\lambda_{H_\alpha\text{StarkFWHM}}$  for different plasma temperatures. It is obvious, as shown in Fig. 4, that the plasma temperature in the range of  $5000\text{--}40000 \text{ K}$  has no significant influence on the dependence of  $N_e$  on  $\Delta\lambda_{H_\alpha\text{StarkFWHM}}$ .

## III. RESULTS AND DISCUSSIONS

### A. Images of Pulsed Discharge Plasma Underwater

The integrated photographs of the pulsed discharge induced underwater in the conditions of the applied peak voltages of  $67$ ,  $72$ , and  $82 \text{ kV}$  are shown in Fig. 5. As observed in Fig. 5, the discharge spread in all directions for all the applied voltages

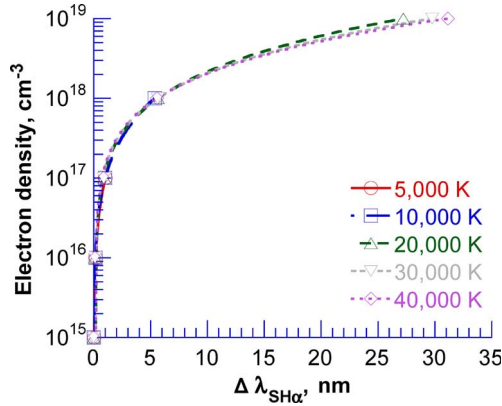


Fig. 4. Relationship between  $N_e$  and  $\Delta\lambda_{H_\alpha\text{StarkFWHM}}$ .

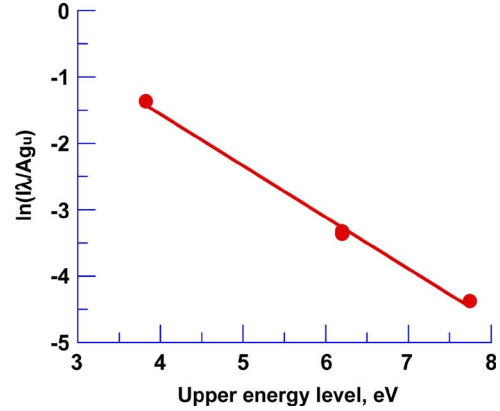


Fig. 7. Boltzmann's plot computed from (1) and Fig. 4.

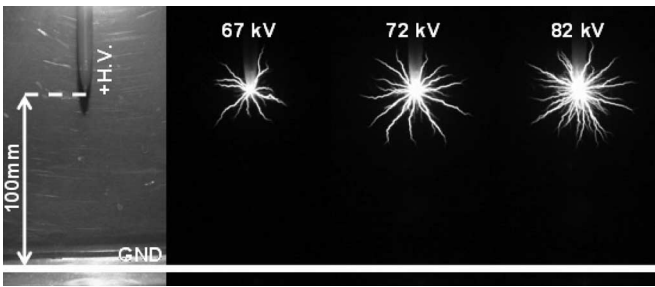


Fig. 5. Discharge images for different applied voltages.

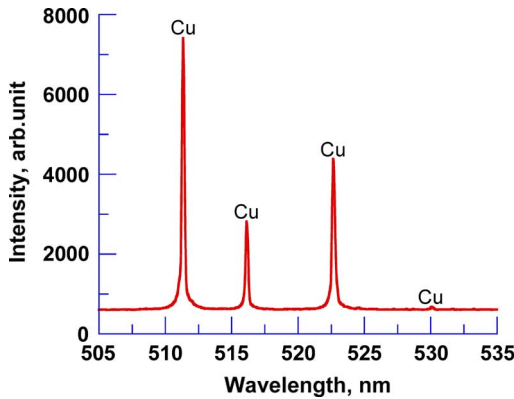


Fig. 6. Four lines of copper spectra emitted from a discharge plasma.

in the range of the maximum applied voltage from 67 to 82 kV. The maximum propagated length of the discharge from the tip of the anode needle was almost the same for the different voltages applied to the needle electrode. On the other hand, the number of discharge channels increased with increasing the applied voltage. This is because the input energy into the electrode increased with the applied voltage resulting in more discharge channels.

**B. Temperature of Pulsed Discharge Plasma Underwater**

Fig. 6 shows the typical time-integrated copper spectra of a discharge emission for 82 kV of peak applied voltage to the needle electrode. In this experiment, the copper needle was utilized as the discharge electrode, and the optical multichannel analyzer was gated for 100 μs from the onset of the applied voltage. Fig. 6 shows that four spectral lines from copper were

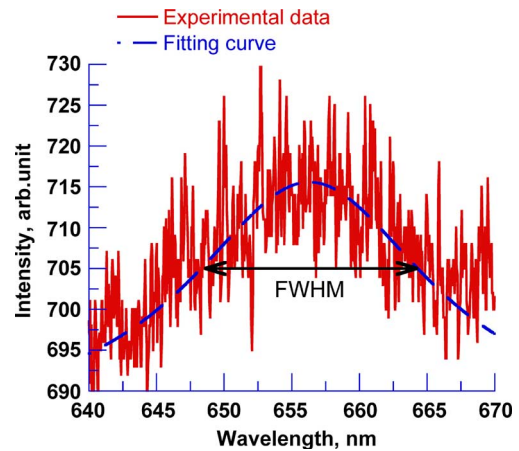


Fig. 8. Typical  $H_\alpha$  spectra broadened by Stark effect.

emitted from the discharge plasma located around the needle electrode. Fig. 7 shows the Boltzmann's plot calculated by (1) and the spectra in Fig. 6. As shown in Fig. 7, it is obvious that the intensity of copper lines (multiplied by wavelength and divided by transition probability and statistical weight) decreases exponentially with the energy of the upper energy level. This result shows that there is a thermal distribution of the electron energies in the discharge plasma produced underwater. In this case, it could be assumed that there is complete thermal equilibrium since the density of the discharge plasma is high enough. From the inclination of the plot in Fig. 7 (= Boltzmann's plot), the plasma temperature was computed to be 15 000 K. This temperature (= 15 000 K) was also calculated for 67 and 72 kV of applied voltage.

**C. Electron Density in Pulsed Discharge Plasma Underwater**

It should be noted that spectral broadening caused by the Doppler effect can be ignored when the plasma temperature is 15 000 K. This is because the Doppler broadening was computed to be less than 0.1 nm in the case of 15 000 K of plasma temperature. The following equation was used in the calculation of the Doppler broadening [3]:

$$\Delta\lambda_D = 2 \left[ \frac{2kT \ln 2}{Mc^2} \right]^{\frac{1}{2}} \lambda_0 \tag{3}$$

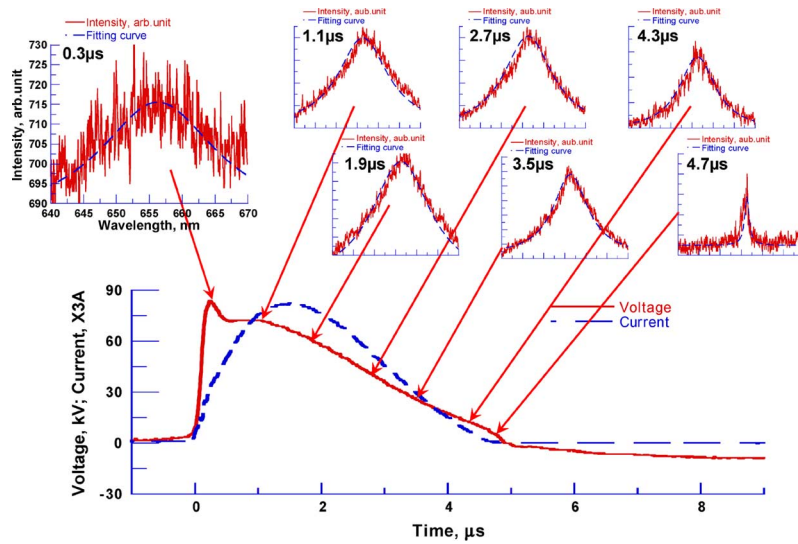


Fig. 9. Dependence of  $H_{\alpha}$  spectra broadened by Stark effect.

where  $\Delta\lambda_D$ ,  $K$ ,  $T$ ,  $M$ ,  $c$ , and  $\lambda_0$  are the broadening width caused by Doppler effect in nanometer, Boltzmann’s constant in joule per kelvin, plasma temperature in kelvin, radiator mass in kilograms per molecule, light speed in meters per second, and unshifted wavelength in nanometer, respectively.

Fig. 8 shows the typical spectra of  $H_{\alpha}$  ( $= 656.3$  nm) mainly broadened by Stark effect. In this case, the gate time of the multichannel analyzer was fixed at 200 ns. To define the FWHM of broadened  $H_{\alpha}$  spectra, the Lorentzian function was used to fit the curve to the spectra measured in the experiment. The Lorentzian function is well known as a main function for Stark broadening and is expressed as follows:

$$I(\lambda) = \frac{A}{(\lambda_0 - \lambda)^2 + (B/2)^2} + C \quad (4)$$

where  $I$ ,  $\lambda$ ,  $\lambda_0$ ,  $A$ ,  $B$ , and  $C$  are the emission intensity, wavelength in nanometer, center wavelength (656.3 nm for  $H_{\alpha}$ ) in nanometer, constant, constant corresponding to the FWHM, and constant, respectively.

Fig. 9 shows the dependence of  $H_{\alpha}$  spectra on time and the waveforms of the applied voltage and discharge current through the electrode. It was seen in Fig. 9 that the Stark broadening was smaller with time. This is because the stored energy in  $C_1$  of MPC decreased with time. Fig. 10 shows the time dependence of electron density in the discharge plasma underwater and the waveforms of the applied voltage and the discharge current in the needle-to-plane electrode for different applied voltages. For all applied voltages, the electron density in the discharge plasma located around the needle electrode exceeded  $10^{18}/\text{cm}^3$  during the initial discharge phase ( $< 4 \mu\text{s}$ ), and then, it decreased quickly with the lower applied voltage and smaller discharge current. This means that an applied voltage to an electrode has no significant influence on the temperature and electron density in a discharge plasma underwater.

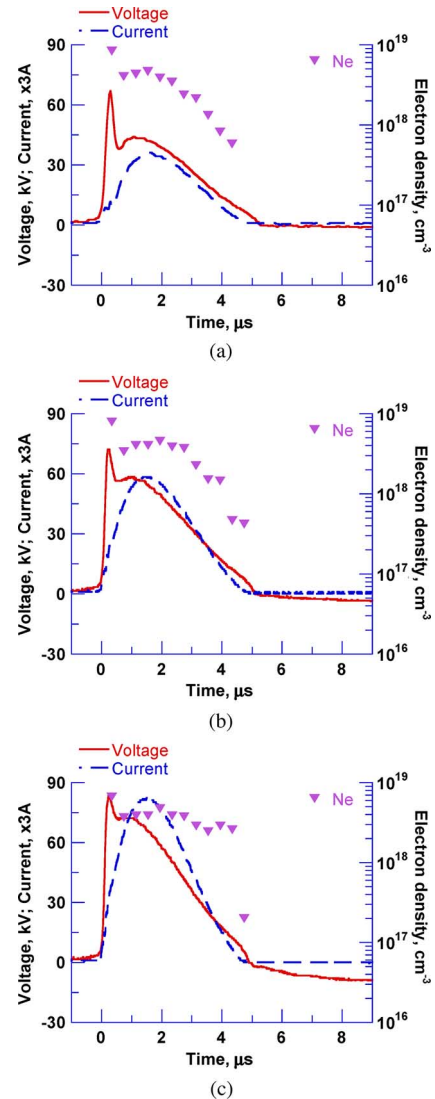


Fig. 10. Time dependence of the electron density for three applied voltages to the electrode. (a) Applied voltage of 67 kV. (b) Applied voltage of 72 kV. (c) Applied voltage of 82 kV.



#### IV. CONCLUSION

An MPC was constructed as a maintenance-free generator for producing a discharge plasma in water. The temperature and electron density in the pulsed discharge plasma induced in water have been calculated by spectroscopic measurements. The following have been deduced.

- 1) A maintenance-free generator based on the MPC circuit was developed to produce the discharge underwater.
- 2) The temperature of the discharge plasma induced in water was calculated to be 15 000 K in case of 67–82 kV of peak applied voltage.
- 3) The electron density of the discharge plasma underwater was estimated to be above  $10^{18}/\text{cm}^3$  during the initial discharge phase in the case of 67–82 kV of peak applied voltage.

#### REFERENCES

- [1] H. Akiyama, "Streamer discharges in liquids and their applications," *IEEE Trans. Dielectr. Electr. Insul.*, vol. 7, no. 5, pp. 646–653, Oct. 2000.
- [2] S. Katsuki, H. Akiyama, A. Abou-Ghazala, and K. H. Schoenbach, "Parallel streamer discharges between wire and plane electrodes in water," *IEEE Trans. Dielectr. Electr. Insul.*, vol. 9, no. 4, pp. 498–506, Aug. 2002.
- [3] T. Namihira, S. Tsukamoto, D. Wang, S. Katsuki, R. Hackam, K. Okamoto, and H. Akiyama, "Production of nitric monoxide using pulsed discharges for a medical application," *IEEE Trans. Plasma Sci.*, vol. 28, no. 1, pp. 109–114, Feb. 2000.
- [4] J. Ashkenazy, R. Kipper, and M. Caner, "Spectroscopic measurements of electron density of capillary plasma based on stark broadening of hydrogen lines," *Phys. Rev. A, Gen. Phys.*, vol. 43, no. 10, pp. 5568–5574, May 1991.
- [5] H. R. Griem, *Spectral Line Broadening by Plasma*. New York: Academic, 1974.



**Takao Namihira** (M'00–SM'05) was born in Shizuoka, Japan, on January 23, 1975. He received the B.S., M.S., and Ph.D. degrees from Kumamoto University, Kumamoto, Japan, in 1997, 1999, and 2003, respectively.

From 1999 to 2006, he was a Research Associate at Kumamoto University, where he is currently an Associate Professor. During 2003–2004, he was on sabbatical leave at the Center for Pulsed Power and Power Electronics, Texas Tech University, Lubbock.



**Shunsuke Sakai** was born in Kumamoto, Japan, on July 22, 1983. He received the B.S. and M.S. degrees from Kumamoto University, Kumamoto, in 2006 and 2007, respectively, where he is currently working toward the Ph.D. degree.



**Takahiro Yamaguchi** was born in Ehime, Japan, on May 23, 1981. He received the B.S. and M.S. degrees from Kumamoto University, Kumamoto, Japan, in 2004 and 2006, respectively.

He is currently with Ishikawajima-Harima Heavy Industries Company, Ltd., Kanagawa, Japan.



**Kunihiro Yamamoto** was born in Kumamoto, Japan, on September 26, 1982. He received the B.S. and M.S. degrees from Kumamoto University, Kumamoto, in 2005 and 2007, respectively.

He is currently with Toray Industries, Inc., Shiga, Japan.



**Chiemi Yamada** was born in Nagasaki, Japan, on February 20, 1984. She received the B.S. degree from Kumamoto University, Kumamoto, Japan, in 2006, where she is currently working toward the M.S. degree.



**Tsuyoshi Kiyan** was born in Okinawa, Japan, in 1965. He received the B.S. degree from the University of Ryukyus, Okinawa, Japan, in 1996 and the M.S. and Dr. Sci. degrees from Kumamoto University, Kumamoto, Japan, in 1998 and 2002, respectively.

He is currently a Research Associate with the 21st Century Center of Excellence (COE) Program on Pulsed Power Science, Kumamoto University.



**Takaishi Sakugawa** received the M.E. degree from Kyushu University, Kyushu, Japan, in 1989 and the D.E degree from Kumamoto University, Kumamoto, Japan, in 2004.

From 1989 to 2004, he was with Meidensha Corporation. He is currently an Associate Professor at Kumamoto University.

Dr. Sakugawa is a member of the Laser Society of Japan, Institute of Electrostatics Japan, and Japan Society of Applied Physics.



**Sunao Katsuki** (M'99) was born in Kumamoto, Japan, on January 5, 1966. He received the B.S., M.S., and Ph.D. degrees from Kumamoto University, Kumamoto, in 1989, 1991, and 1998, respectively.

From 1991 to 1998, he was with Kumamoto University as a Research Associate, where he is currently an Associate Professor. During 2001–2002, he was a Senior Researcher in the Plasma and Electronics Research Institute, Old Dominion University, Norfolk, VA.



**Hidenori Akiyama** (M'87–SM'99–F'00) received the Ph.D. degree from Nagoya University, Nagoya, Japan, in 1979.

From 1979 to 1985, he was with Nagoya University as a Research Associate. Since 1985, he has been with the faculty of Kumamoto University, Kumamoto, Japan, where he is currently a Professor.

Dr. Akiyama received the IEEE Major Education Innovation Award in 2000 and the IEEE Peter Haas Award in 2003.